Investigations of microscopic magnetic properties of the pseudo-binary system $(Zr_{1-x}Ti_x)Fe_2$

2003 J. Phys.: Condens. Matter 15 6403

(http://iopscience.iop.org/0953-8984/15/37/008)

INSTITUTE OF PHYSICS PUBLISHING JOURNAL OF PHYSICS: CONDENSED MATTER

J. Phys.: Condens. Matter **15** (2003) 6403–6414 PII: S0953-8984(03)65465-2

Investigations of microscopic magnetic properties of the pseudo-binary system $(Zr_{1-x}Ti_x)Fe_2$

Z Surowiec[1], M Wiertel[1], A I Beskrovnyi[2], J Sarzyński[1] and J J Milczarek[3]

[1] Institute of Physics, M Curie-Skłodowska University, M Curie-Skłodowska 1, 20-031 Lublin, Poland
[2] Frank Laboratory of Neutron Physics, Joint Institute for Nuclear Research, 141980 Dubna, Russia
[3] Institute of Atomic Energy, Świerk, 05-400 Otwock, Poland

Received 30 June 2003
Published 8 September 2003
Online at stacks.iop.org/JPhysCM/15/6403

Abstract

The magnetic structure and hyperfine interactions in the polycrystalline pseudo-binary system $(Zr_{1-x}Ti_x)Fe_2$ for $x \leqslant 0.2$ and $x \geqslant 0.7$ were studied using the techniques of neutron diffraction and the Mössbauer effect. The results of our measurements reveal the cubic C15 and the hexagonal C14 crystal structure for low and high Ti atom concentration x, respectively. For the ferrimagnetic region of the C15 structure the reduction from 1.58(5) to 1.30(6) μ_B of Fe magnetic moments with increasing x at room temperature was found. The presence of two hyperfine magnetic fields in the antiferromagnetic C14 phases suggests the existence of small magnetic moments on Fe atoms at 2a in addition to those present at the 6h sites. The magnetic structure refinement for the $(Zr_{0.3}Ti_{0.7})Fe_2$ alloy yielded magnetic moments perpendicular to the c axis of 0.19(10) μ_B at Fe 2a sites at 10 K. The results confirm the spin-canted antiferromagnetic structure with a canting angle of 8° at 10 K in the pseudo-binary phase.

1. Introduction

The studies of ternary alloys such as $(A_{1-x}A'_x)B_2$ are very important and technologically useful because their electrical, magnetic, optical and structural properties can be tailored by changing the concentration x. The changes of the magnetic (ferro–antiferro) and crystalline structure (cubic–hexagonal) occurring in the $(Zr_{1-x}Ti_x)Fe_2$ system with changes in the Ti atom concentration and temperature are very interesting.

In this paper we present the results of investigations carried out on $(Zr_{1-x}Ti_x)Fe_2$ alloys at different temperatures by means of Mössbauer spectroscopy and neutron diffractometry. The alloys form the pseudo-binary Laves phases in which Ti atoms replace a part of Zr atoms. Such a substitution is possible due to the similar atomic sizes of Ti and Zr atoms (1.46 and 1.60 Å, respectively) as well as to their chemical similarity (Pauling electronegativities 1.3

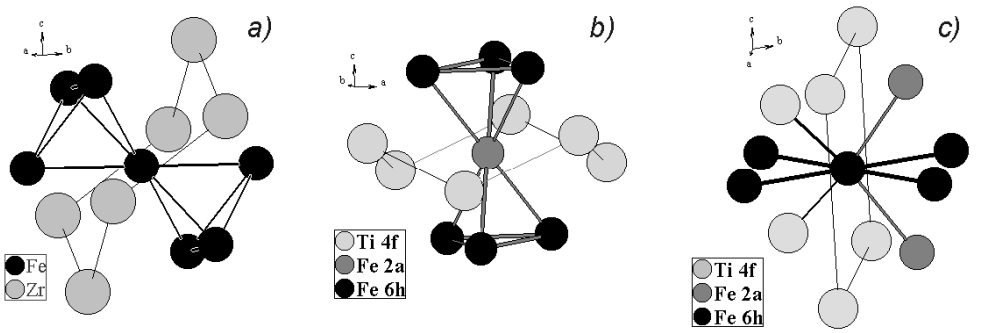

Figure 1. The nearest neighbours of the Fe atom at: (a) I or II site in the C15 structure, (b) 6h and (c) 2a sites of the C14 structure.

and 1.2, respectively). Another possibility is the formation of a mixture of both cubic and hexagonal phases in one sample. Powder x-ray diffractograms were made for samples in the full concentration range confirming a single phase of the C15 structure in the compounds with Ti content less than 0.20 and a single phase of the C14 structure in the probes with Ti content $x > 0.7$. Powder patterns in a range of the Ti concentration $0.2 < x < 0.7$ show the coexistence of both phases [1]. Here we focus our attention on the regions of pure phase only. This temporary limitation is due to the complications encountered in the mixed phase region.

The $ZrFe_2$ compound is a ferromagnet ($T_C = 630$ K, $M_S(\mathrm{RT}) = 76$ emu g^{-1} [2]) with a magnetic moment of about 1.6 μ_B at each Fe atom at room temperature (RT). The neutron diffraction measurement results [3] reveal also an antiparallel induced magnetic moment of about -0.3 μ_B at Zr sites as a result of the hybridization of 3d Fe and 4d Zr bands [4]. The Laves phase $TiFe_2$ is an antiferromagnet ($T_N = 285$ K [5]). More detailed magnetic properties will be discussed in section 3.2 of this paper.

In the cubic C15 type ($MgCu_2$, space group $Fd\bar{3}m$) phase Fe atoms form regular tetrahedra (16d positions of the $\bar{3}m$ point symmetry) connected via their corners. Six Fe and six Zr atoms surround each Fe atom forming its nearest neighbours (see figure 1(a)). In the hexagonal C14 type ($MgZn_2$, space group $P6_3/mmc$) phase Fe atoms form the sublattice of regular tetrahedra linked alternately by their apexes (2a positions of the $\bar{3}m$ point symmetry) or by their bases (6h positions of the mm point symmetry). The population ratio of 6h and 2a sites is equal to 3:1. The number of the nearest neighbours of Fe atoms is identical to that in the C15 structure. The difference between the structures consists in different local symmetry of the nearest neighbour positions (see figures 1(b) and (c)). In the C15 structure all Fe atoms have local $\bar{3}m$ symmetry with a threefold axis along one of the [111] directions.

For the intermetallic $ZrFe_2$ the [111] axis is also the magnetic moments ordering axis. However, in the presence of a magnetic field the principal axis of the electric field gradient (EFG) can take two different positions, one along the [111] direction and the other inclined at 70° 32′ to that axis. This effect distinguishes two types of magnetically non-equivalent Fe positions called I and II respectively, with a population ratio of 3:1.

In the C14 structure the principal axes of the local EFGs for 6h sites are perpendicular to the c axis as an easy magnetization axis. In the case of 2a sites relevant axes overlap. The iron atoms create a triangular Kagomé lattice which favours topological frustration. Both this frustration and the magnetic instability of the iron moments should contribute to the frustrated magnetic arrangements. In the pseudo-binary Laves phase compounds the situation is even more complicated. A small substitution of Ti atoms for A atoms in $(A_{1-x}Ti_x)Fe_2$ phases

changes the iron–iron distances, the topological frustration and, finally, destabilizes the iron magnetic ordering. Some types of these pseudo-binary phases have been reported to show a spin canting [6, 7]. It is also known [8, 9] that in the C14 phase the thermal fluctuations of the 6h Fe moments give rise to a dynamical molecular field on 2a sites at a temperature close to T_N, which causes strong spin fluctuations and an emerging magnetic moment at these sites. The easy magnetization axes may change their direction [10], yielding a wide range of possible angles θ between them and the EFG tensor principal axes. This pattern is observed in the relevant Mössbauer spectra showing different values of quadrupole shifts $\varepsilon_Q = QS(3\cos^2\theta - 1)/2$, where $QS = e^2qQ/4$.

The aim of our work was to investigate in detail a magnetic arrangement in $(Zr_{1-x}Ti_x)Fe_2$ for low and high Ti concentrations x.

2. Experimental details

The pseudo-binary $(Zr_{1-x}Ti_x)Fe_2$ compounds in polycrystalline form were prepared by arc melting appropriate stoichiometric amounts of zirconium, titanium and iron of 4N purity, in an argon atmosphere. To avoid inhomogeneities the samples were remelted several times. The crystal structure of the samples produced was examined by x-ray diffraction with Cu Kα radiation ($\lambda = 1.5406$ Å) at Θ–2Θ geometry. The ^{57}Fe Mössbauer spectra (MS) of the powdered samples were measured using a constant acceleration spectrometer in transmission mode with the ^{57}Co/Rh source. For both phases the sextet intensity ratio (6h sites/2a sites or I sites/II sites) was fixed as 3:1. All other parameters were set free in the fitting processes. The isomer shift (IS) values are given with respect to α-Fe. For measurements at different temperatures centre shifts (CS) containing the second-order Doppler shift (SOD) contribution are presented ($CS(T) = IS + SOD$).

The neutron diffraction (ND) experiments were performed with the DN2 time-of-flight powder diffractometer at the fast pulsed reactor IBR-2 in the Frank Laboratory of Neutron Physics, Joint Institute for Nuclear Research (JINR), and with the TKSN 420 triple-axis spectrometer operated in elastic mode at a neutron wavelength of 0.986 Å at the Institute of Atomic Energy, Świerk. The diffraction patterns were refined by the FULLPROF Rietveld refinement program [11]. A convolution of the pseudo-Voigt with the double exponential function was chosen to generate the line shape of the diffraction peaks. In the final run the following parameters were refined from the ND data: scale factor, background coefficients, unit-cell parameters, pseudo-Voigt parameter, positional coordinates, isotropic thermal factors and the magnitude of the Fe ordered magnetic moments. The coherent scattering lengths for Fe, Ti and Zr were taken as 9.45, −3.44 and 7.16 fm, respectively.

3. Results and discussion

3.1. Neutron diffraction and Mössbauer spectra studies for the low Ti concentration

Neutron scattering measurements were performed at several fixed temperatures between 290 K (room temperature) and 670 K for $(Zr_{1-x}Ti_x)Fe_2$ samples with $x \leqslant 0.20$.

A section of the neutron powder diffraction patterns obtained with the DN2 diffractometer for the $(Zr_{0.9}Ti_{0.1})Fe_2$ compound at 290 and 670 K is presented in figure 2.

The pattern at 670 K (figure 2(a)) is characteristic of the nuclear Bragg reflections associated with the $MgCu_2$-type structure and was used to refine the structural parameters. In figure 2 the full curves represent the calculated pattern, the points are the experimental data and the lower curves are the difference between the observations and the fits. Excellent agreement with a reliability factor of about 4% is obtained.

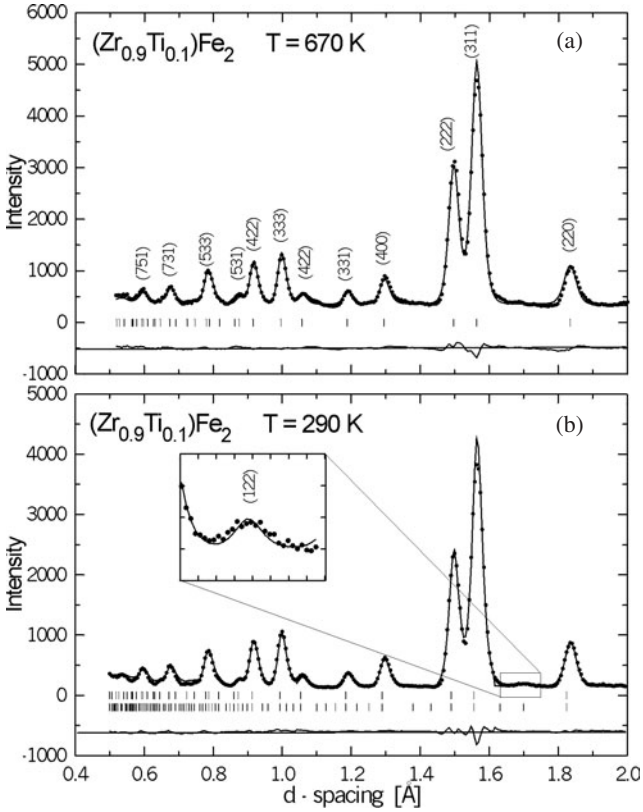

Figure 2. The neutron spectra measured by means of the DN2 diffractometer for $(Zr_{0.9}Ti_{0.1})Fe_2$ compounds at: (a) 670 K and (b) 290 K. The full curves represent the calculated pattern, the points the observed one and the lower curves the difference between observations and calculations. Short vertical lines below the diffraction pattern indicate the calculated nuclear Bragg positions (upper row), and the magnetic ones (lower row). The magnetic peak is shown in the inset.

Below the Curie temperature (figure 2(b), $T = 290$ K), the patterns are characterized by an increase of the intensity of some Bragg peaks due to a magnetic contribution to the diffraction pattern. This is most clearly observed for the (122) reflection at $d = 1.7$ Å, which is shown in the inset of figure 2(b). The other magnetic peaks were not distinctly observed as separate because they overlap with nuclear Bragg reflections.

The diffraction patterns were refined using the full Rietveld method. For the $(Zr_{0.9}Ti_{0.1})Fe_2$ compounds we found a magnetic moment of about 1.58 μ_B at RT for Fe atoms and an antiparallel induced small magnetic moment at Zr sites of about $-0.32(4)$ μ_B. These observations are consistent with the magnetic structure proposed by Warren *et al* [6].

The magnetic moments for $(Zr_{0.8}Ti_{0.2})Fe_2$ at the Fe 16d sites are found to be 1.3 and -0.12 μ_B at the Zr 8a sites. A summary of the results of the refinements for $(Zr_{1-x}Ti_x)Fe_2$ compounds with $x = 0.1$, 0.15 and 0.20 for a few temperatures is given in table 1.

The patterns were refined assuming the magnetic moments ordering axis along one of the [111] directions for the C15 phase. The thermal variation of the lattice parameters obtained from the neutron diffraction show a nearly linear increase with increasing temperature. About 2% decrease of the cubic cell dimension in the C15 phase region is related to the partial substitution of Zr atoms by smaller Ti atoms without structure transformation. Only minor deviations from Vegard's law are observed.

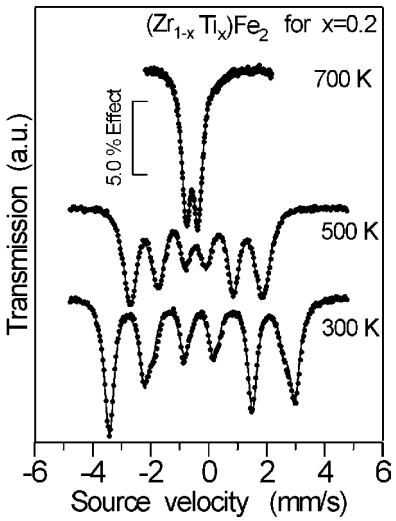

Figure 3. The Mössbauer spectra for $(Zr_{0.8}Ti_{0.2})Fe_2$ collected at different temperatures.

Table 1. Summary of the refined parameters for $(Zr_{1-x}Ti_x)Fe_2$, with $x = 0.1, 0.15, 0.2$.

			Moment (μ_B)	
x	T (K)	Lattice constant a (Å)	μ_{Fe}	μ_{Zr}
0.10	670	7.099(2)	—	—
	370	7.077(2)	1.40(4)	−0.27(4)
	290	7.054(3)	1.58(5)	−0.32(4)
0.15	670	7.082(2)	—	—
	400	7.045(2)	1.03(5)	−0.18(3)
	290	7.050(3)	1.38(5)	−0.20(4)
0.20	650	7.045(2)	—	—
	400	7.044(2)	0.93(6)	−0.12(5)
	290	7.044(3)	1.30(6)	−0.12(4)

The replacement of Zr atoms by Ti atoms in the cubic structure yields a decrease in the magnetic moments and a reduction in the Curie temperature.

Additional and more detailed information can be obtained from the conventional Mössbauer spectra measured for $(Zr_{1-x}Ti_x)Fe_2$ for $x \leqslant 0.2$ in the temperature range between 300 and 700 K (figure 3). The spectra were fitted with two subspectra with the fixed intensity ratio 3:1 corresponding to the ratio of sites I and II in the C15-type structure. From the fit for $ZrFe_2$ at 300 K the hyperfine magnetic fields (HMFs) B_{hf} of 20.3(2) and 19.1(2) T at sites I and II, respectively, were estimated.

The temperature dependencies of the hyperfine interaction parameters extracted from the numerical analysis of corresponding spectra for $(Zr_{0.8}Ti_{0.2})Fe_2$ are presented in figure 4. Two curves in figure 4(a) showing the temperature dependence of the HMF values result from the occurrence of two magnetically non-equivalent positions of ^{57}Fe probes. It is known [12] that in weak itinerant ferromagnets the self-consistent renormalization (SCR) theory predicts a temperature dependence for magnetization M of $M(T) \propto (T_C^{4/3} - T^{4/3})^{1/2}$. However, the analysis of the B_{hf} ($\propto M$) behaviour in the temperature interval from RT to the Curie point exhibits an

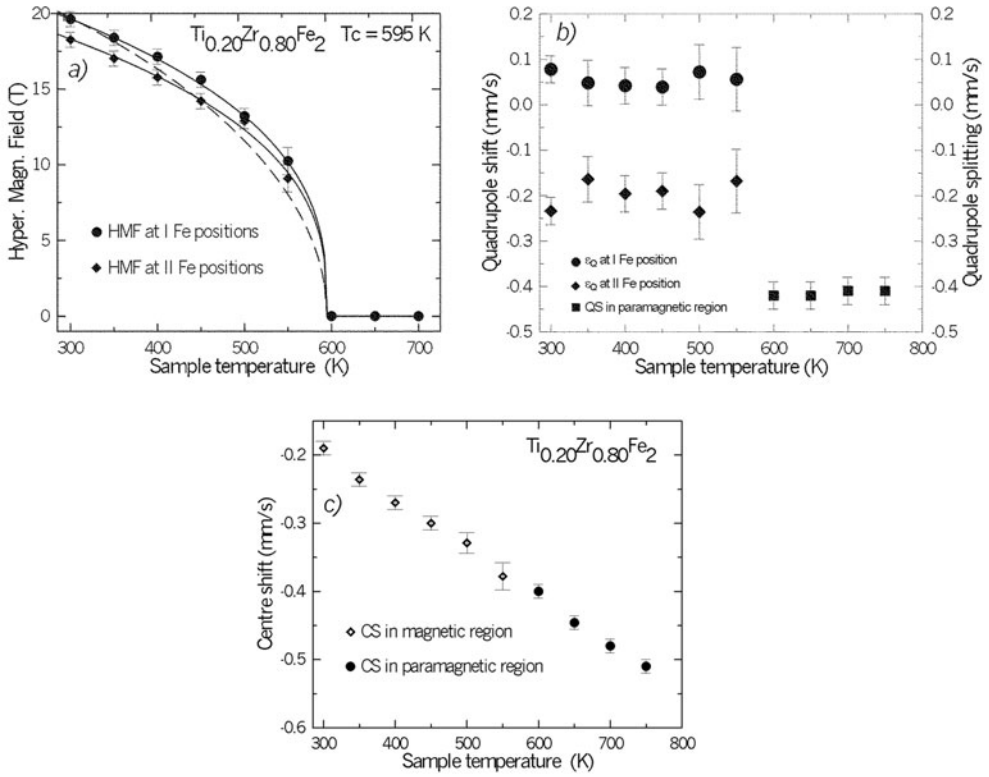

Figure 4. Temperature dependence of: (a) the HMF (●—site I, ♦—site II; the solid curves are fits according to the expression $B_{\mathrm{hf}} \propto (T_{\mathrm{C}} - T)^{\beta}$; the dashed curve represents the $T^{4/3}$ law), (b) the quadrupole splitting or the quadrupole shift (QS) ε_{Q} and (c) the centre shift (CS) for $x = 0.2$.

experimental dependence well described by the commonly used function $B_{\mathrm{hf}} \propto (T_{\mathrm{C}} - T)^{\beta}$, with β being the critical exponent for temperatures close to the Curie temperature and equal to 0.35(4). Hence we can determine the Curie temperatures by extrapolation of the B_{hf} curve to the zero field, as equal to about 595(8) K for the $(Zr_{0.8}Ti_{0.2})Fe_2$ alloy and about 625(6) K in the $(Zr_{0.9}Ti_{0.1})Fe_2$ sample. T_{C} for pure $ZrFe_2$ reaches 630(6) K and is exactly the same as in [2]. Our investigations indicate that the HMF decreases slightly with increasing Ti concentration and a reduction in the value of T_{C} is observed. It seems that the classification of $(Zr_{1-x}Ti_x)Fe_2$ for $x \leqslant 0.2$ as a weak itinerant ferromagnet is called into question by the temperature dependence of the HMF.

As shown in figure 4(b), in the paramagnetic range the QS remains almost constant and is equal to $-0.42(3)$ mm s^{-1}. Similarly the QS values for both I and II Fe positions do not reveal clear dependence on temperature. From this experimental fact it follows that the angles θ between the principal axes and the easy magnetization axes is independent of temperature. It is interesting to note that the replacement of Zr atoms with Ti atoms does not influence essentially the values or the dependence character of the QS in the concentration range discussed.

The CS values are nearly identical for both components (see figure 4(c)). They change linearly with an increase of the sample temperature and become more negative. This tendency holds above the Curie temperature. Such temperature dependence can be fully explained as a result of the SOD effect.

The IS value at room temperature changes almost monotonically with x from -0.18 mm s^{-1} for pure $ZrFe_2$ to -0.28 mm s^{-1} for pure $TiFe_2$. In the case of the ^{57}Fe probe the s electron density on the nucleus increases. Possible explanations of this concentration dependence are as follows. Firstly, the density of the 4s conduction electrons may increase directly due to the decrease of the nearest neighbour distances. Secondly, the density of the inner 3s Fe electrons may increase as a result of the weaker shielding of these electrons by the 3d Fe electrons. It is known [13] that when 4d transition atoms A are substituted by 3d atoms in the pseudo-binary Laves AFe_2 compound, hybridization between the 3d Fe bands and the d bands of the A atom becomes stronger. Then the width of the Fe 3d band becomes larger and the degree of the states localization in such a band decreases.

3.2. Measurements for the high Ti concentration

Neutron measurements were made as a function of temperature between 10 and 350 K for the $(Zr_{1-x}Ti_x)Fe_2$ samples with $x \geqslant 0.70$. The diffraction patterns were registered for a detector at an angle of 170° to the incoming beam to obtain better resolution. No phase other than the C14 hexagonal structure was detected from the analysis of neutron measurements. Excellent agreement was obtained between the observations and the calculations for all powder diffraction data. The reliability factor was not larger than 4%.

The spectra of $(Zr_{1-x}Ti_x)Fe_2$ for $x \geqslant 0.7$ are significantly different from those for the low content of Ti discussed in the previous subsection and are shown in figure 5. They are characteristic of the C14-type structure. The bottom panel of this figure shows the pattern obtained for $(Zr_{0.3}Ti_{0.7})Fe_2$ measured at $T = 10$ K. The analogous spectra for $x = 1$ are shown in the upper panel. Nuclear and magnetic reflections are marked with short vertical lines. Refinement was performed as in the previous cases. The pattern for $x = 0.7$ differs in intensity for some Bragg reflections from this for $TiFe_2$. An insignificant shift between these spectra results from the change of lattice parameters. This change results from the partial substitution of Ti atoms by Zr atoms which causes the increase of this volume.

The lattice constants for $(Zr_{1-x}Ti_x)Fe_2$ estimated from the ND patterns collected at different temperatures are presented in figures 6(a) and (b). The anomalous anisotropic thermal properties of the lattice constants are clearly visible. The c parameter increases slowly along with decreasing temperature. This trend is observed in the range of occurrence of the magnetic arrangement for all the investigated samples. Above T_N the c parameter increases with increasing temperature. The a parameter decreases versus temperature over the whole temperature range. However, discernible discontinuity was observed in the vicinity of phase transition. Some discontinuity was also observed in the thermal variation of the unit-cell volume (see figure 6(c)). This effect is evidence of a significant magnetostriction effect for these compounds.

The powder ND patterns at 10 K were collected in the d spacing range from 1.2 to 4.4 Å to obtain the maximum number of nuclear reflections. Part of the patterns between 2.15 and 2.40 Å shown in figure 7 at a large scale shows clearly the disappearance of the purely magnetic (111) reflection with increasing temperature. The (103) reflection has a smaller intensity in $TiFe_2$ in comparison with the same reflection in $(Zr_{0.3}Ti_{0.7})Fe_2$ (see figure 5). It is related to the coherent scattering length values for Ti and Zr. The absence of other magnetic peaks not overlapping the Bragg reflections confirms that the magnetic unit cell is commensurate with the crystallographic unit cell. The occurrence of (111) reflection and the absence of the other purely magnetic $P6_3/mmc$ structure reflections (001) and (003) indicate that Fe 6h moments in $TiFe_2$ are aligned antiferromagnetically along the c axis. In such a magnetic structure Fe atoms at 2a sites carry no magnetic moments and the magnetic moments

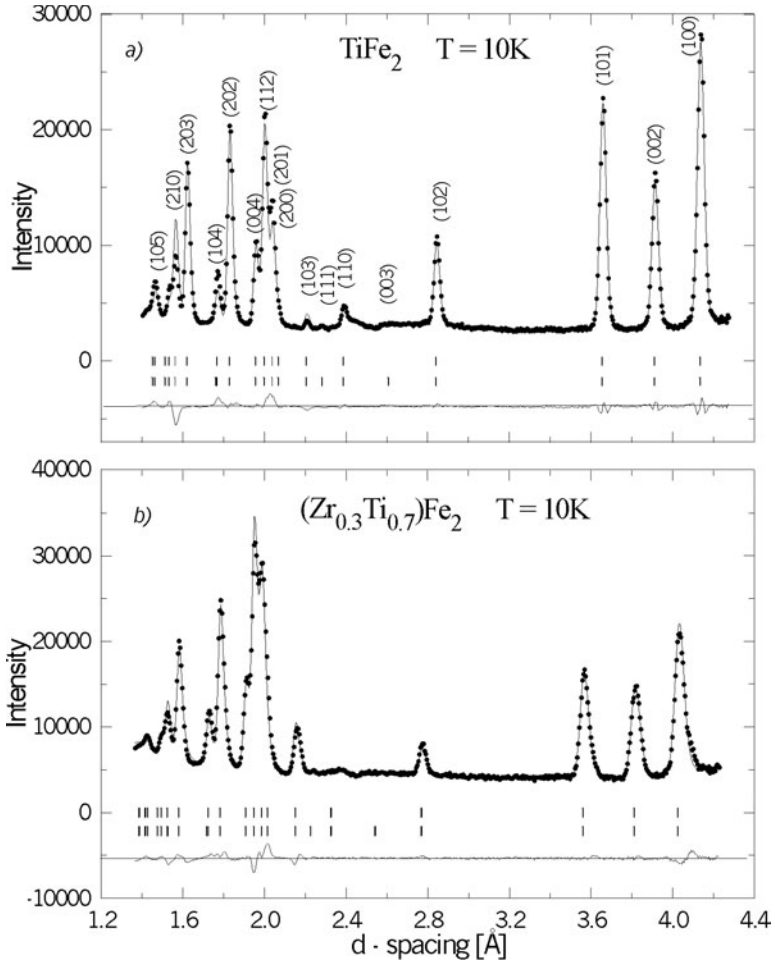

Figure 5. Neutron spectra measured by means of the DN2 diffractometer at 10 K for $(Zr_{0.3}Ti_{0.7})Fe_2$ and $TiFe_2$ compounds. The full curves represent the calculated pattern, the points the observed one and the lower curves the difference between observations and calculations. Short vertical marks below the diffraction pattern indicate the calculated nuclear Bragg positions (upper row) and the magnetic ones (lower row).

of Fe atoms at the 6h sites are ferromagnetically coupled in the layers perpendicular to the *c* axis while the coupling between the adjacent layers is antiferromagnetic [8].

Our previous Mössbauer measurements for the pseudo-binary samples $(Zr_{1-x}Ti_x)Fe_2$ [1] indicate the existence of the HMF at Fe 2a sites. This fact suggests a ferromagnetic arrangement of magnetic moments residing on those sites. On the basis of these results we took an initial model for the magnetic refinement in the $(Zr_{0.3}Ti_{0.7})Fe_2$ phase. We assumed that there is a ferromagnetic component on Fe 6h sites in the basal plane, while the antiferromagnetic components remain parallel to the *c* axis. It should be noted that the existence of a basal plane ferromagnetic component results in a non-zero molecular field at the 2a site. An ordered Fe moment might therefore be expected at the 2a site in the spin-canted phase. The symmetry breaking related to the spin canting does not seem to be large because reflections of type $(00l)$, with odd l, were not observed. However, when the temperature of the pseudo-binary sample decreases below the Néel point (310 K), the integrated intensity of the (002) reflection

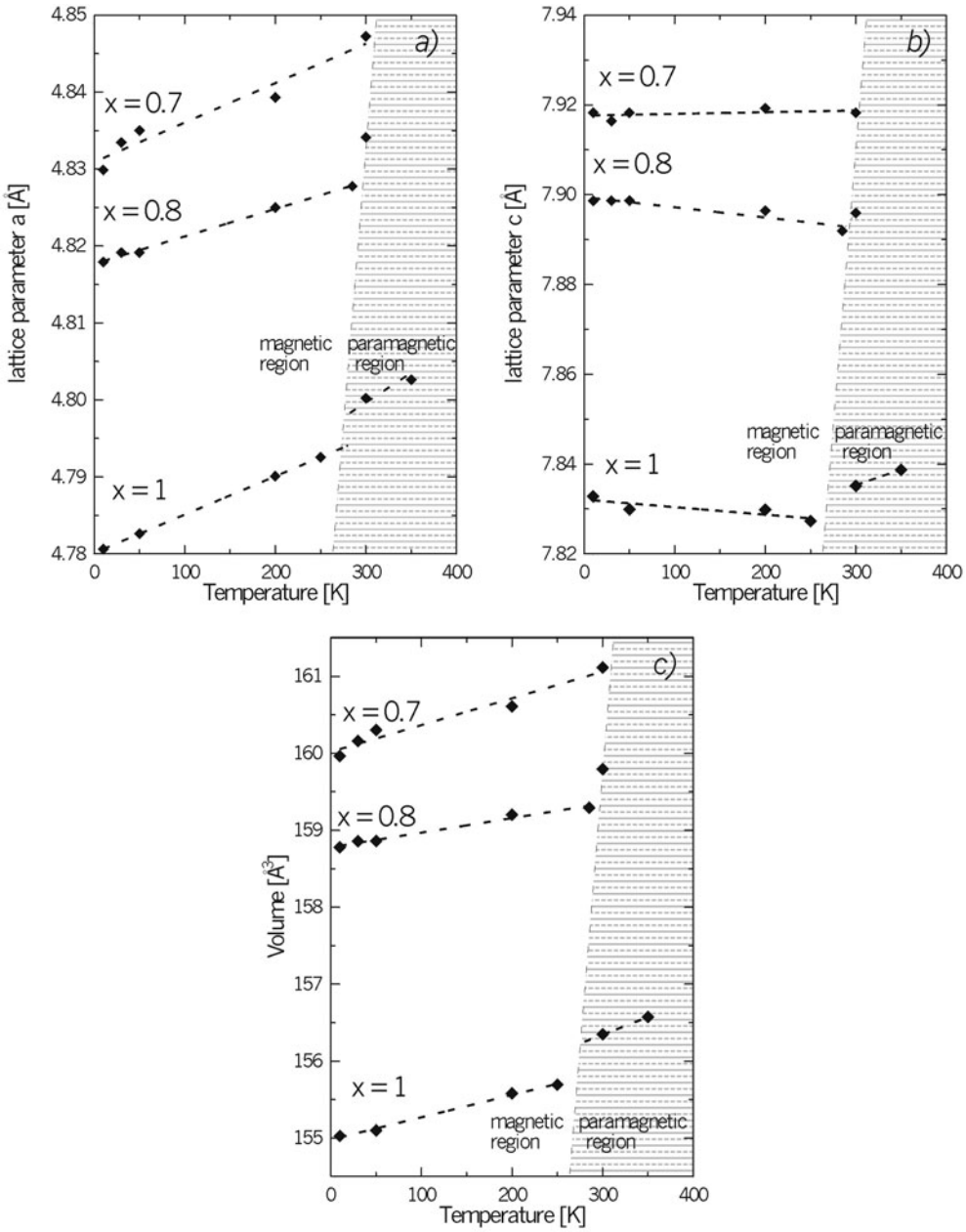

Figure 6. The temperature dependencies deduced from powder ND data for: (a) a parameter; (b) c parameter; (c) unit-cell volume.

noticeably increases. For such a canted magnetic moments arrangement the R magnetic factor values were found to be significantly lower than those for the simple antiferromagnetic model.

The results of the Rietveld refinement for $(Zr_{1-x}Ti_x)Fe_2$, with $x = 1.0$ and 0.7, are collected in table 2. We obtained magnetic moments for Fe atoms at 6h sites in pure $TiFe_2$ equal to 1.2(1) μ_B at 10 K in good agreement with the value given in [8]. The values of the respective magnetic moments in the sample with $x = 0.7$ at 6h sites are about 13% larger.

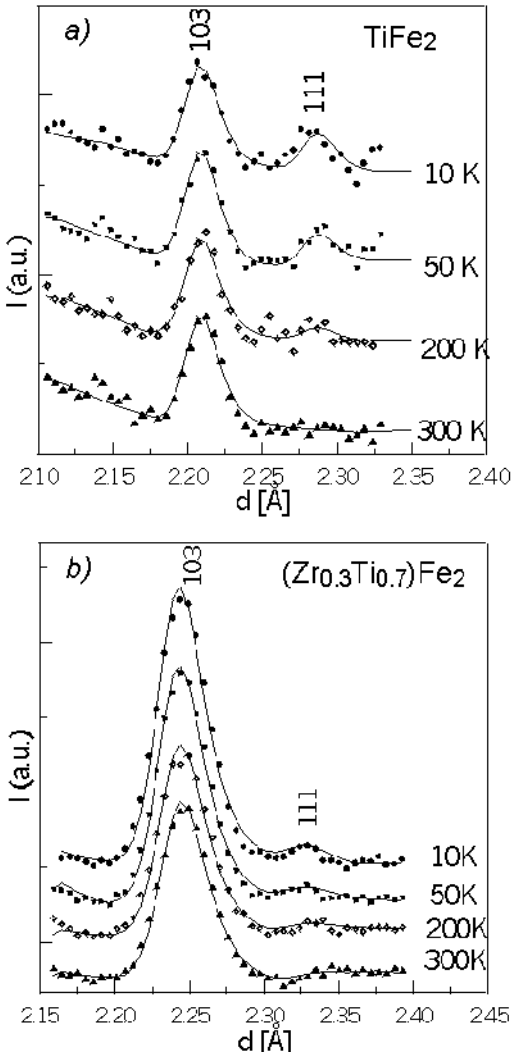

Figure 7. A section of powder ND patterns for $(Zr_{0.3}Ti_{0.7})Fe_2$ and $TiFe_2$ compounds.

Table 2. Summary of Rietveld refinements for the magnetic moments μ_{Fe} and the Mössbauer parameters for $(Zr_{1-x}Ti_x)Fe_2$, with $x = 1.0$ and 0.7.

X	T (K)	CS (6h) (mm s^{-1})	CS (2a) (mm s^{-1})	B_{hf}(6h) (T)	B_{hf}(2a) (T)	μ_{Fe}(6h) (μ_B)	μ_{Fe}(2a) (μ_B)
1.0	10	−0.15	−0.17	9.73(1)	—	1.2(1)	—
	300	−0.26	−0.28	—	—	—	—
0.7	10	−0.10	−0.11	10.4(1)	1.5(3)	1.32(10)	0.19(10)
	300	−0.24	−0.26	4.8(1)	0.4(3)	0.56(8)	0.05(4)

Since the spin canting in the investigated phases has not been unambiguously confirmed by our results of ND measurements, the Ti-rich compounds were studied also by means of the Mössbauer effect. The respective Mössbauer spectra are shown in figure 8. The full curves

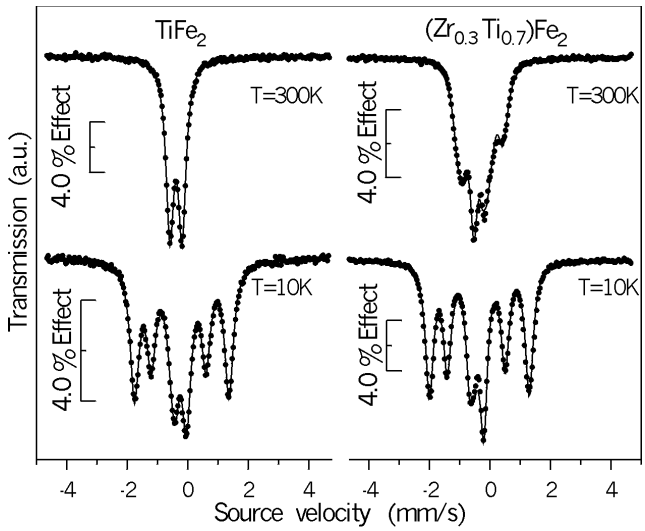

Figure 8. The Mössbauer spectra for $TiFe_2$ (left) and for $(Zr_{0.3}Ti_{0.7})Fe_2$ (right) at 10 and 300 K, respectively.

in the figure were obtained from computer fits. Allowing, as previously, for non-zero fields at both sites and taking into account the relevant sextet intensities, we could assign them to ^{57}Fe atoms at 6h and 2a positions in the hexagonal phase. For $x \geqslant 0.90$ the absence of the HMF results from the paramagnetic character of the samples. The HMF values obtained are given in table 2. For every x concentration and temperature the CS at the 2a site is larger than that of 6h sites by about 0.02 mm s^{-1}. In the case of the ^{57}Fe probe the s electron density on the nucleus increases. For both types of sites the CS decreases with increasing x at constant temperature due to the unit-cell expansion (see figure 6(c)). On the basis of our results and the C14 structure symmetry described earlier, we can draw a conclusion that in spite of different local symmetries of the Fe 2a and 6h sites, the QSs at both these positions have the same value of about $-0.40(3)$ mm s^{-1} which is only slightly dependent on temperature and Ti concentration x. In this case and also for low Ti concentration the negative sign was determined by comparison with the spectra obtained below the ordering temperature.

By a comparison of the magnitude of the magnetic moments with the HMF on the Fe atoms we obtained the hyperfine coupling constant $A \sim 8.1(7)T/\mu_B$. This value is the same for both types of sites. From this fact and the ND results, one could conclude that the ferromagnetic component of Fe 6h magnetic moments is equal to the ferromagnetic component of Fe 2a moments in the coexistent ferro- and antiferromagnetic states. The Mössbauer spectrum observed for $(Zr_{0.3}Ti_{0.7})Fe_2$ was fitted well with one kind of the hyperfine field at 6h sites. Therefore, it is clear that the ferromagnetic component is perpendicular to the antiferromagnetic one. If the ferromagnetic moment is parallel to the antiferromagnetic one, two different hyperfine fields should be observed at the 6h site. The total moment at the 6h sites cants over to the ferromagnetic direction. The canting angle θ_c is determined as the angle between the total 6h moment and the direction of its antiferromagnetic component. It is 0° in the antiferromagnetic state and 90° in the ferromagnetic state. The angle θ_c determined from the hyperfine fields at 6h and 2a sites is small, equal to about 8° at 10 K and decreases to about 5° at 300 K. The changes in the magnetic moment at 2a sites cannot be interpreted in terms of the localized spin model. The magnetic state of this system should be explained as the

coexistent state of ferro- and antiferromagnetism in the itinerant electron system. Therefore, it is concluded that the magnetic structure at low temperature for $x = 0.7$ is the perpendicular overlapped state of the ferromagnetic and antiferromagnetic spin densities. It seems that the disorder induced by replacement of Zr atoms with Ti atoms leading to symmetry breaking of the exchange field causes the spin canting in the compound under discussion.

4. Conclusions

The neutron diffraction and Mössbauer spectroscopy experiments described here have provided the first direct observation of the spin structure in the pseudo-binary $(Zr_{1-x}Ti_x)Fe_2$ compounds. The complementary application of both experimental techniques resulted in a detailed discussion of magnetic moments arrangements in the investigated alloys. The alloys of the system are ferromagnetic for $x = 0.2$, antiferromagnetic for $x = 1.0$ and spin-canted antiferromagnetic for the $0.7 \leqslant x < 1.0$ region. The spin canting angle θ_c estimated from the hyperfine field values at 6h and 2a sites amounts to about 8° at 10 K.

The magnetostriction effect is clearly observed in the temperature dependencies of the unit-cell volumes.

Generally, our investigations confirm the suggestion that the spatial disorder present in the phases with high Ti concentration resulting from Ti replacement with Zr atoms and the phase interaction may have a similar effect on the magnetic structure as the thermal fluctuations of the 6h Fe moments.

Acknowledgments

The authors would like to thank Professor K Tomala for many helpful discussions and Mr R Kmieć for the Mössbauer measurements at low temperature.

References

[1] Budzyński M, Sarzyński J, Surowiec Z and Wiertel M 2001 *Acta Phys. Pol.* A **100** 717
[2] Muraoka Y, Shiga M and Nakamura Y 1979 *J. Phys. F: Met. Phys.* **9** 1889
[3] Warren P, Forsyth J B, McIntyre G J and Bernhoeft N 1992 *J. Phys.: Condens. Matter* **4** 5795
[4] Crook M R, Colest B R, Ritter C and Cywinski R 1996 *J. Phys.: Condens. Matter* **8** 7785
[5] Yamada Y, Kitaoka Y, Asayama K and Sakata A 1984 *J. Phys. Soc. Japan* **53** 3634
[6] Nishihara Y and Yamaguchi Y 1985 *J. Phys. Soc. Japan* **54** 1122
[7] Terao K and Shimizu M 1987 *Phys. Status Solidi* b **139** 485
[8] Brown P J, Deportes J and Oualaddiaf B 1992 *J. Phys.: Condens. Matter* **4** 10015
[9] Nishihara Y and Yamaguchi Y 1983 *J. Phys. Soc. Japan* **52** 3630
[10] Wiesinger G, Oppelt A and Buschow K H J 1981 *J. Magn. Magn. Mater.* **22** 227
[11] Rodriguez J, Anne M and Pannetier J 1987 *Institute Laue–Langevin Report* 87R014T p 5795
[12] Masuda Y 1983 *J. Magn. Magn. Mater.* **31–34** 259
[13] Asano S and Ishida S 1988 *J. Phys. F: Met. Phys.* **18** 501